Applied Geochemistry 101 (2019) 75–87

Contents lists available at ScienceDirect

Applied Geochemistry

journal homepage: www.elsevier.com/locate/apgeochem

Development of ion exchangers for the removal of health-hazardous perchlorate ions from aqueous systems

Dorota Kołodyńska[a,*], Paulina Hałas[a], Rajmund Michalski[b]

[a] Department of Inorganic Chemistry, Faculty of Chemistry, Maria Curie-Skłodowska University, M. Curie Skłodowska Sq. 2, 20-031, Lublin, Poland
[b] Institute of Environmental Engineering, Polish Academy of Sciences, Sklodowska-Curie 34 Street, 41-819, Zabrze, Poland

ARTICLE INFO

Editorial handling by Eric M Pierce

Keywords:
Perchlorates
Chelating resin
Polymeric ligand exchanger
Diffusion mechanisms
Kinetic models

ABSTRACT

In order to investigate diffusion models and adsorption mechanism of polymeric ligand exchangers (PLE) for the removal of perchlorate from tap water Lewatit MonoPlus TP 220-Cu, Lewatit MonoPlus TP 220-CuEDDS, Dowex 4195-Cu and M 4195-CuEDDS were prepared and compared with commercial Lewatit TP 220 and Dowex M 4195. Based on the adsorption experiments, diffusion mechanisms were studied using the intraparticle diffusion, film diffusion, Boyd, Dumwald-Wagner models. The pore diffusion coefficient (D_p), film diffusion coefficient (D_f) as well as well-known kinetic models like the pseudo first and the pseudo second order were also applied to fit the experimental data. The adsorption study was carried out at pH equal 7.0 and different contact time. The kinetics of adsorption was based on the pseudo second order model. The adsorption studies show that the adsorption rate controlling step is realized mainly by intraparticle diffusion. The basic surface structural changes before and after the perchlorate sorption on each sorbent were investigated using ATR-FTIR. After sorption the band at 1085 cm^{-1} appeared which showed efficiency of the sorption process. The adsorbents were also characterized by the nitrogen adsorption/desorption isotherms, thermogravimetry (TG) and derivative thermogravimetry (DTG) analysis. The study proved efficiency of Lewatit MonoPlus TP 220-Cu and Lewatit MonoPlus TP 220-CuEDDS, Dowex 4195-Cu and M 4195-CuEDDS for perchlorate removal from water.

1. Introduction

Perchlorate ions (ClO_4^-) occur naturally as well as man-made components. Natural occurrence is related to O_3 oxidation of Cl^- in dry and semi-dry locations. The reaction of O_3 and Cl^- is slow, however, that process is very important due to the natural ample occurrence of O_3 and Cl^-. The tetrahedron structure and high activity of perchlorate cause that the oxidizing power is deferred. All in all, natural formation, chemical stability and optional discharge make perchorate widespread (Jiang et al., 2017; Urbansky, 1998; Ye et al., 2012). The synthetic presence of perchlorate is found in fireworks, rocket propellants, ammunitions, fertilizers, air bag inflators and matches production. High solubility and poor adsorption of perchlorate lead to its detection in surface and ground water as well as in food, milk, fish, drinking water and edible plant species. It was confirmed that large amounts of perchlorate could have negative effects on human bodies. It can interfere with the uptake of iodine (Tang et al., 2013; Yao et al., 2017). In view of negative impact on human health and environment impact there were introduced standards for perchlorate. The official reference dose of perchlorate (RfD) was made to be as 0.7 μg/kg a day by the National Academy of Sciences (NAS). Whereas the United States Environmental Protection Agency (US EPA) proposed a drinking water equivalent level (DWEL) of 24.5 μg/dm^3 and in 2008 published the level of perchlorate in drinking water called health advisory level (HAL) of 15 μg/dm^3 (Asami et al., 2013; Yao et al., 2017) Such low concentration levels require appropriate methods for determination of contaminants.

Ion chromatography is a recognized technique applied for determination of perchlorate in both drinking water and other sources. There are several methods introduced and approved by the US EPA. They consist in ion chromatography with conductivity detection and suppression. In 1997 there was developed a method called 314.0 using the Dionex Ion Pac AS5 column with the detection limit (DL) 0.53 μg/L and the minimum reporting level (MRL) of 4.0 μg/L (Office EPA, 1999). As for method 314.1 perchlorate ions are introduced to the concentrator column and then eluted to the guard and analytical Dionex Ion Pac AS20 columns. The lowest concentration minimum reporting level (LCMRL) for perchlorate on the AS20 column was defined to be 0.13 μg/dm^3 with DL 0.03 μg/dm^3 (Pohl et al., 2005). This method was improved in 2009. In 2005 two other methods were published (331.0 and 332.0). They use the liquid chromatography electrospray ionization

* Corresponding author.
E-mail address: d.kolodynska@poczta.umcs.lublin.pl (D. Kołodyńska).

https://doi.org/10.1016/j.apgeochem.2018.12.025
Received 24 November 2017; Received in revised form 18 December 2018; Accepted 21 December 2018
Available online 23 December 2018
0883-2927/

Abbreviations

NAS	National Academy of Sciences
LD	detection limit
DWEL	drinking water equivalent level
HAL	health advisory level
LCMRL	lowest concentration minimum reporting level
LC	liquid chromatography
LC/ESI/MS	liquid chromatography electrospray ionization mass spectrometer
MDL	method detection limit
MRL	minimum reporting level
RfD	reference dose
US EPA	United States Environmental Protection Agency
SIM	selected ion monitoring
MRM	multiple reaction monitoring
SBA	strongly basic anion exchanger
WBA	weakly basic anion exchanger
CIE	chelating ion exchanger
PLE	polymer ligand exchanger
TP220	Lewatit MonoPlus TP 220
M 4195	Dowex M 4195
ZPC	zero point of charge

mass spectrometer (LC/ESI/MS). Method 331 used liquid chromatograpy LC column Dionex Ion Pac AS21 and 200 mM CH_3NH_2 as a mobile phase. The DL was 0.005 μg/dm^3 for selected ion monitoring or 0.008 μg/dm^3 for multiple reaction monitoring detection, while LCMRL – 0.022 μg/dm^3 or 0.056 μg/dm^3 (Wendelken et al., 2005). In 332.0 method LD was equal to 0.02 μg/dm^3 and LCMRL 0.1 μg/dm^3 (Hendrick et al., 2005).

Ion exchange also proved to be the most effective method for perchlorate removal from drinking water on a large scale (Xie et al., 2016a). In the group of ion exchangers the following should be mentioned:

- quaternary ammonium strongly basic anion exchangers (SBA) of type I (trimethylammonium), type II (dimethylhydroxoethylammonium) and type (III) (tripropylammonium),
- weakly basic anion exchangers (WBA),
- chelating ion exchangers (CIE) used as polymer ligand exchangers (PLE).

It has been proved that along with the increase of the length of hydrocarbon chain of the functional group, the selectivity toward perchlorate ion increases. However, its total exchange ability and the rate of ion exchange reaction decrease. These phenomena can be explained by an increase of the hydrophobic nature of the functional group with increasing its size as well as hindered diffusion of higher molecular weight amines into the polymer structure during incorporation of the functional groups to the matrix. Also one can find the decrease of the rate of ions diffusion to the functional groups of ion exchanger with the increasing chain length of the functional group.

Of the group of chelating ion exchangers Dowex M 4195 and Lewatit MonoPlus TP 220 can be applied. The chelating resin Dowex M 4195 manufactured by the Dow Chemical Company is a weak base with a polystyrene matrix and bis(2-pyridylmethyl)amine also known as a bis(picolylamine) functional group. Its advantage is possibility of transition metals separation from acidic solutions (Diniz et al., 2005; Kołodyńska, 2010). It is widely used as a sorbent for chromium(VI) (Saygi et al., 2008), copper (Janin et al., 2009), nickel and cobalt (Mendes and Martins, 2004; Nagib et al., 1999) as well as lead (Diniz et al., 2005; Zhang and Cheng, 2007) ions.

Lewatit MonoPlus TP 220 produced by Lanxess can be used also as a sorbent for copper (Kołodyńska et al., 2014), palladium, gold and platinum (Wołowicz and Hubicki, 2012). In the case of perchlorate removal the chelating ion exchangers Lewatit MonoPlus TP 220 and Dowex M 4195 should be used as polymeric ligand exchangers (PLE). The basis for creation of PLE is the presence of bis(picolylamine) functional group attached to the macroporous polystyrene divinylbenzene copolymer matrix which is in the metal ion form. It is well-known that this group is capable of forming complexes with most metal ions in the second oxidizing state like Cu(II), Ni(II), Zn(II), Co(II), Fe(II) as well as Fe(III) and Cr(III). The presence of cations results in the interactions between them and their functional groups with donor atoms (Janin et al., 2009). However, the studies presented in (Henry et al., 2004) show that Cu(II) was chosen as the most stable Lewis acid metal. Zhao and Sengupta (1998) proposed the PLE model referred to Dowex M 4195 by loading Cu(II) ions for selective phosphate(V) removal. Moreover, Tao et al. (2011) proposed PLE as a sorbent for arsenate(V) ions removal.

In this study Lewatit MonoPlus TP 220 and Dowex M 4195 were used to prepare the polymeric ligand exchangers by loading Cu(II) ions and Cu(II)-EDDS complexes. In our previous paper it was proved that M 4195 is very useful for simultaneous removal of Cu(II) ions and EDDS anions. Therefore these commercial ion exchangers were used to determine the possibility of perchlorate sorption and removal from aqueous solutions. The obtained results were adjusted to several diffusion and kinetic models.

2. Material and methods

2.1. Preparation of adsorbents and adsorbates

Dowex M 4195 (Dow Chemical Company) and Lewatit MonoPlus TP 220 (Lanxess) were washed with methanol, 1 M HNO_3 in acetone, 1 M NaOH and deionized water before being used. In the paper they are denoted as M 4195 and TP 220. Their physicochemical properties are presented in Table 1. Additionally, the polymeric ligand exchangers obtained by sorption of Cu(II) ions or Cu(II)-EDDS complexes on Lewatit MonoPlus TP 220 and Dowex M 4195 were used for perchlorate removal in the presence of Cl^-, Br^-, NO_3^-, PO_4^{3-} and SO_4^{2-} ions.

Table 1
Some physicochemical properties of Lewatit MonoPlus TP 220 and Dowex M 4195 as well as based on the polymeric ligand exchangers (PLE) obtained by sorption of Cu(II) and Cu(II)-EDDS.

Ion exchanger	TP 220	TP220-Cu	TP220-CuEDDS	M 4195	M 4195-Cu	M 4195-CuEDDS
Matrix structure	PS-DVB	PS-DVB	PS-DVB	PS-DVB	PS-DVB	PS-DVB
BET surface area (m^2/g)	19.98	24.08	25.32	–	–	–
Form	OH^-	Cu^{2+}	$Cu(EDDS)^{2-}$	SO_4^-	Cu^{2+}	$Cu(EDDS)^{2-}$
Moisture content (%)	48.0–60.0	–	–	40.0–60.0	–	–
Colour	white	black	bright green	brown	black	dark green

PS-DVB = polystyrene-divinylbenzene.

They are denoted as M 4195-Cu and M 4195-CuEDDS as well as TP220-Cu and TP220-CuEDDS. Ethylenediamine-N,N′-disuccinic acid (EDDS) belongs to the group of new biodegradable complexing agents and forms complexes with metal ions in the M(II):EDDS = 1:1 system. Therefore EDDS (Innospec Speciality Chemicals, UK) was used as supplied to react with appropriate solutions of these metal ions at pH without adjustment. The stock Cu(II) solution was further diluted to the required experimental concentration i.e. 1×10^{-3} M. The initial pH of the solution was 4.2 for Cu(II). The other chemicals were of analytical grade. The basic characteristics of the above mentioned ion exchangers are also presented in Table 1.

The initial solution of perchlorate (1000 mg/dm^3) (Sigma-Aldrich) was prepared using ultra-pure water. The suitable concentration of perchlorate (10 mg/dm^3) for the kinetic studies was obtained from tap water to ensure typical concentrations of Cl^-, Br^-, NO_3^-, PO_4^{3-}, SO_4^{2-} ions.

The ions concentrations were determined by ion chromatography 940 Professional IC Vario (Metrohm) with the Metrosep A SUPP5 column (250/4.0 mm) and the suppressed conductivity detector. 100 mM H_2SO_4 was used for suppressor regeneration. As the eluent 35% acetonitrile and water solution of 20 mM Na_2CO_3 were applied. During the determination procedure the following parameters were used: pressure 11.2 MPa, temperature 46.1 °C and eluent flow rate 0.7 cm^3/min. Fig. 1 shows the chromatograms of standards 1–3 containing ClO_4^- ions with the presence of Cl^-, Br^-, NO_3^-, PO_4^{3-}, SO_4^{2-} ions typical of tap water. The elution time of the above-mentioned conditions is 9.98 min for Cl^-, 8.65 min for Br^-, 9.02 min for NO_3^-, 11.4 min for PO_4^{3-}, 11.84 min for SO_4^{2-} ions and 20.1 min for ClO_4^-

2.2. Characterization of adsorbents

FTIR spectrometer with the monolithic diamond crystal Cary 630 (Agilent Technologies) was used to record the ATR-FTIR spectra before and after perchlorate sorption on M 4195, M 4195-Cu, M 4195-CuEDDS, TP 220, TP 220-Cu and TP 220-CuEDDS. The attenuated total reflectance (ATR) is a single-reflection ATR. Infrared spectra were recorded in the range of 4000-650 cm^{-1}.

ASAP 2405 (Micromeritics Instrument Co., Norcross, USA) was used for measuring the specific BET surface area and average pore diameter of the studied ion exchangers before and after perchlorate sorption.

Thermogravimetric analyses of the studied polymers were performed using the TG/DTG techniques at a heating rate of 0–1000 °C/min in the N_2 atmosphere using TA Instruments Q50 TGA.

The surface charge of sorbents (pH_{zpc}) was estimated by the titration method. 0.5 g of dry sample of the ion exchanger was suspended in a reaction vessel with 50 cm^3 of distilled water with three ionic backgrounds 0.1 M, 0.01 M and 0.001 M NaCl. The suspension was stirred using a magnetic stirrer and 0.1 M HCl or 0.1 M NaOH was added for titration. The analytical set of precise titration Dosino, Titrando (Metrohm) was applied in order to compare the obtained results. The zero point of charge (pH_{zpc}) was also determined by the drift method. The ionic background was 0.01 M NaCl solution at pH 2–12.

2.3. Batch adsorption studies

The batch kinetic studies were carried out in 100 cm^3 conical flasks at the phase contact time changing from 1 to 180 min. 0.05 g of resin and 20 cm^3 of the initial solutions of perchlorate at the concentration equal to 10 mg/dm^3 with tap water were placed in flasks. The samples were shaken with 7 amplitude on the mechanical shaker (Elpin Plus, Poland) at room temperature. The solutions pH was measured by the pH meter pHM82 (Radiometer Copenhagen, Netherlands).

The uptake of perchlorate q_t (mg/dm^3) was calculated using Eq. (1):

$$q_t = V(c_0 - c_t)/m \quad (1)$$

where: c_0 is the initial concentration of the solution (mg/dm^3), c_t is the solution concentration after time t (min), V is the volume of the solution (dm^3), m is the dry weight of the adsorbent (g).

2.4. The sorption percentage %S (%)

$$\%S = (c_0 - c_t)/c_0 \times 100\% \quad (2)$$

where: c_0 is the initial concentration of the solution (mg/dm^3), c_t is the solution concentration after time t (min).

2.5. Adsorption mechanism and kinetic models

In order to study the mechanism and actual rate controlling step in the sorption of perchlorate ions there were discussed the following kinetic and diffusion models: pseudo first order, pseudo second order, intraparticle diffusion, film diffusion, Boyd, Dumwald-Wagner. The pore diffusion (D_p) and the film diffusion (D_f) coefficients were also calculated.

The pseudo first order model is presented in the following form:

$$dq_t/dt = k_1(q_e - q_t) \quad (3)$$

This equation can be transformed to the linear form (Eq. (4)):

$$\log(q_e/q_e - q_t) = k_1 t/2.303 \quad (4)$$

$$\log(q_e - q_t) = \log(q_e) - k_1 t/2.303 \quad (5)$$

where: q_t is the amount of perchlorate adsorbed at time t (mg/g), q_e is the amount of perchlorate adsorbed at equilibrium (mg/g), k_1 is the rate constant of the pseudo first order model (1/min).

The line plots of $log(q_e\text{-}q_t)$ vs. t for perchlorate sorption are useful to calculate the rate constants and correlation coefficients (Ho and Mckay, 1998).

The other kinetic model is the pseudo second model presented as:

$$dq_t/dt = k_2(q_e - q_t)^2 \quad (6)$$

This equation can be transformed to the linear form (Eqs. (7) and (8)):

$$1/q_e - q_t = 1/q_e + k_2 t \quad (7)$$

$$t/q_t = 1/k_2 q_e^2 + t/q_e \quad (8)$$

The plots of t/q_t vs. t were also tested to obtain rate parameters and correlation coefficients. Both the pseudo first and pseudo second order

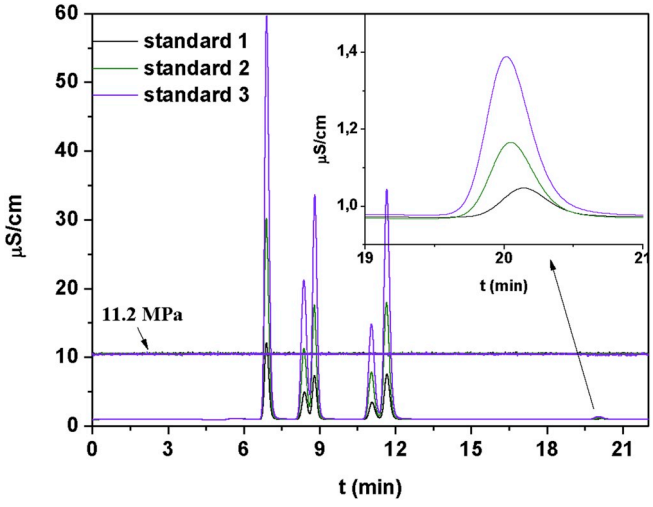

Fig. 1. The chromatograms of ClO_4^- standards with the presence of typical for tap water ions: Cl^-, Br^-, NO_3^-, PO_4^{3-}, SO_4^{2-}. The analytical conditions: detection – suppressed conductivity, temperature 46.1 °C and 0.7 cm^3/min eluent flow rate.

models are widely used to evaluate the sorption processes (El-Khaiary et al., 2010).

However, as these two kinetic models can not identify the diffusion mechanism the intraparticle diffusion model (IPD) also called the Weber and Morris kinetic model (W-M) was used to this end and presented as:

$$q_t = k_i t^{1/2} + C \quad (9)$$

where: C is the intercept, k_i is the intraparticle diffusion rate constant (mg/g $min^{1/2}$).

It is well-known that if the plots of q_t vs. $t^{1/2}$ are linear and pass through the origin of the system, the intraparticle diffusion is the rate controlling step affecting adsorption (Ho and Mckay, 1998; Khalil et al., 2016). But if the plots do not pass through the origin, the intraparticle diffusion is not the rate limiting step. Based on this model thickness of the boundary layer can be also determined. In this case the rate of adsorption can be controlled by other kinetic models simultaneously.

Then the data were analyzed by the kinetic expression given by the Boyd model (BM):

$$F = q_t/q_e = 1 - 6/\pi^2 \exp(-Bt) \quad (10)$$

$$Bt = -0.4977 - \ln(1 - F) \quad (11)$$

where: q_t is the amount of perchlorate ions adsorbed at time t, q_e is the amount of perchlorate ions adsorbed per g of resin at equilibrium (mg/g), Bt is the mathematical function of F which is the fraction of solute adsorbed at time t (fractional attainment of equilibrium at time t).

The Boyd model was proposed for the ion exchange kinetics and is widely applied in numerous papers to determine the rate controlling step (Kiruba et al., 2014; Nethaji et al., 2013; Viegas et al., 2014). The values of D_i parameter called the effective diffusion coefficient were calculated at different initial concentrations using Eq. (12):

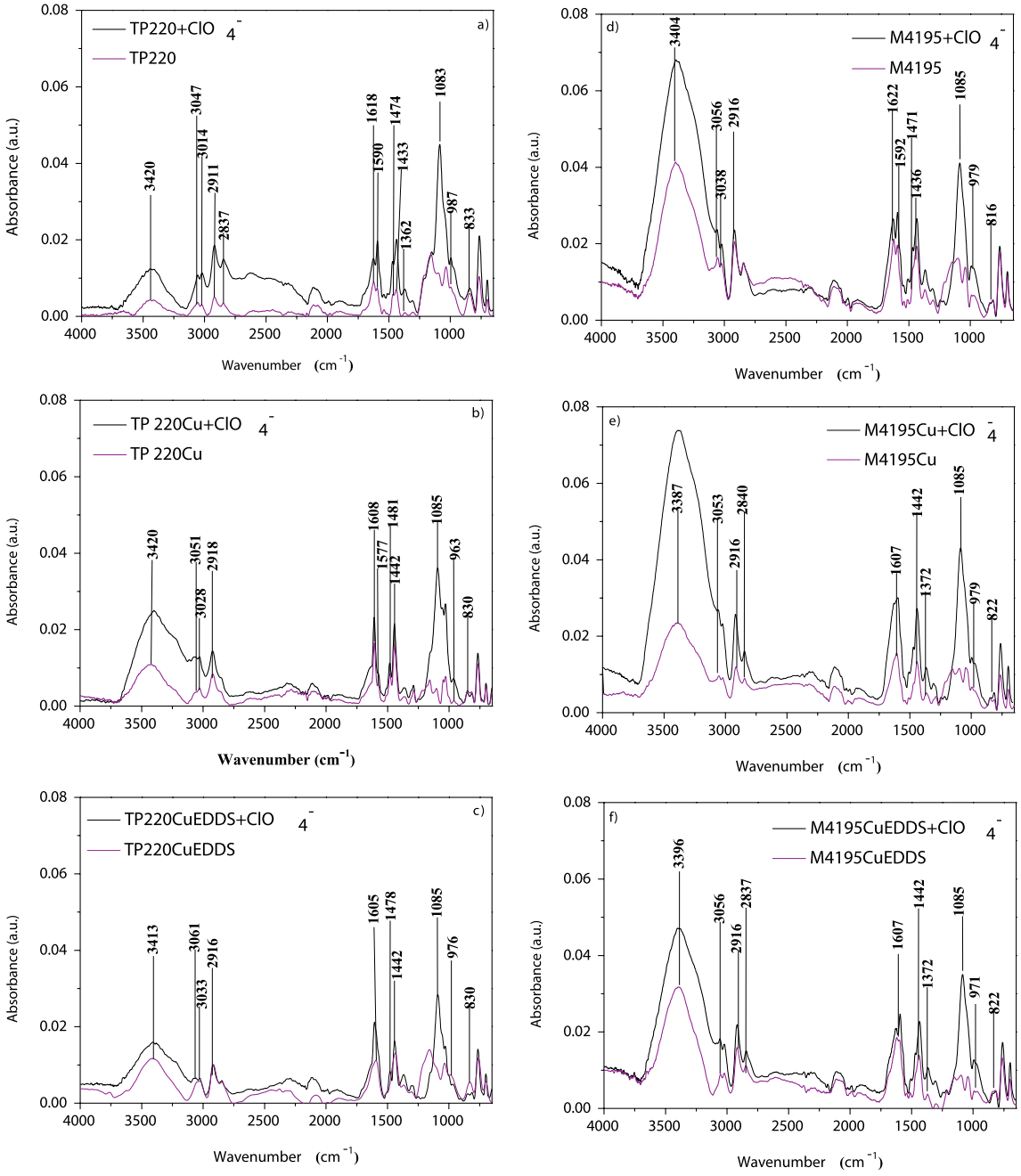

Fig. 2. ATR-FTIR spectra before and after perchlorate ions sorption on a) TP 220, b) TP 220-Cu, c) TP 220-CuEDDS, d) M 4195, e) M 4195-Cu and f) M 4195-CuEDDS.

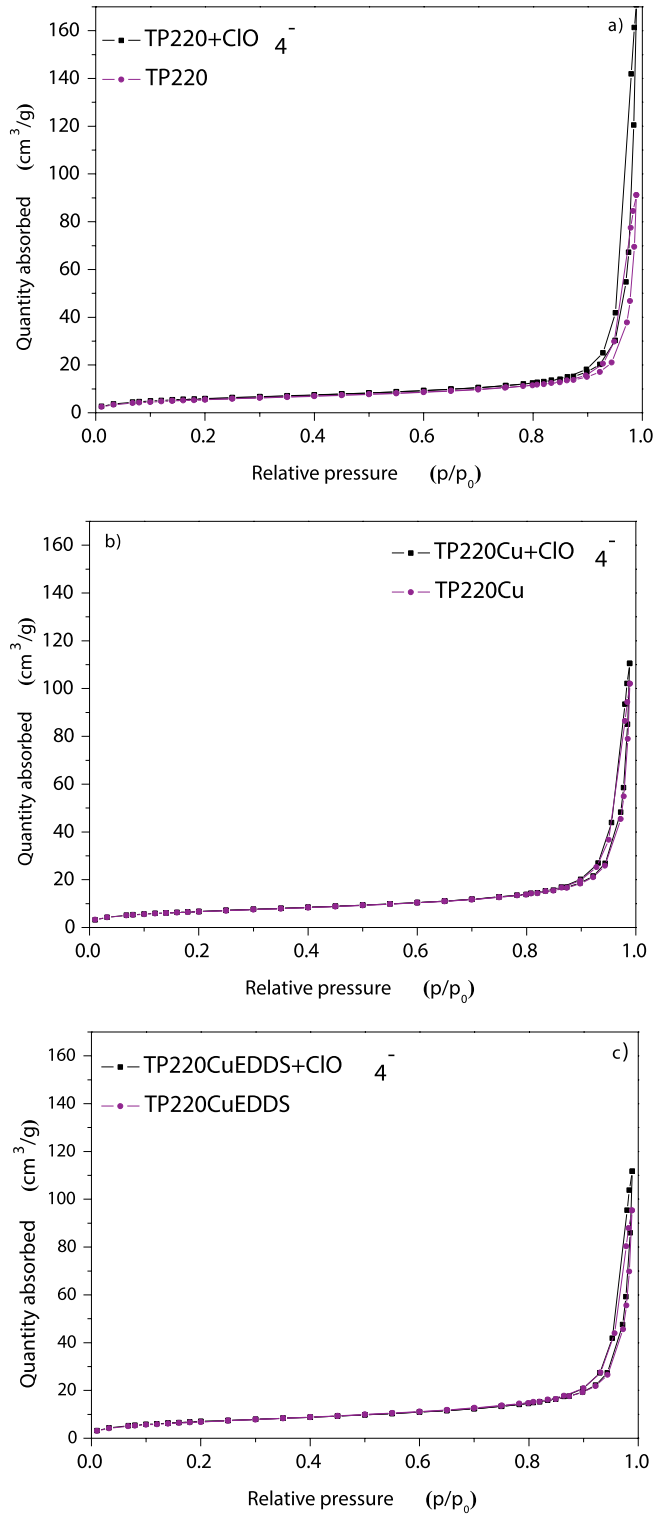

Fig. 3. N_2 adsorption/desorption isotherms and pore width distributions of a) TP 220 b) TP 220-Cu and c) TP 220-CuEDDS.

$$B = \frac{\pi^2 D_i}{r^2} \tag{12}$$

where: r is the radius of the resin particles (m), D_i (m^2/s) is the effective diffusion coefficient (Viegas et al., 2014).

The plot Bt vs. t is a straight line passing through the origin if the diffusion coefficient (D_i) does not change with F.

The Dumwald-Wagner model (D-W) was proposed for investigations of reactions of a solid phase produced with spherical particles of uniform radius and a gaseous phase. The diffusion into or out of the solid phase is the slowest step in the process. Besides, this model proved to be useful in solid reactions (Flor et al., 1974). Generally, the Dumwald-Wagner model can be applied for description of solid-liquid phase adsorption and was employed for Cu(II) ions sorption on the bagasse pulp cellulose (Zhu et al., 2015). The mathematical model of Dumwald-Wagner equation is:

$$F = q_t/q_e = 1 - 6/\pi^2 \sum_{n=1}^{\infty} \frac{1}{n^2} \exp(-n^2 kt) \tag{13}$$

where: k (1/min) is the rate constant referring to adsorption. The simplified Dumwald-Wagner equation can be represented as follows:

$$\log(1 - F^2) = -kt/2.303 \tag{14}$$

The rate k can be obtained from the slope of a linear plot $log(1\text{-}F^2)$ vs. t (Faccini et al., 2016a; Hai et al., 2012).

The film diffusion model (FD) equation is presented below:

$$\ln(1 - F) = -k_f t \tag{15}$$

where: k_f is the film diffusion rate (1/min), F is defined as previously (Bai et al., 2016).

In order to assess character of the diffusion process, the pore diffusion (D_p) and the film diffusion (D_f) coefficients were also calculated:

$$D_p = 0.03r^2/t_{1/2} \tag{16}$$

$$D_f = 0.23r\delta q_e/t_{1/2}c_0 \tag{17}$$

where: r is the radius of the ion exchanger (cm), δ is the film thickness equal to 0.001 (cm), q_e is the amount of perchlorate sorbed at equilibrium (mg/g), C_o is the initial concentration (mg/dm^3), $t_{1/2}$ is the time when the half of maximum sorption capacity is obtained (s).

3. Results and discussion

3.1. Characteristics of ion exchangers and polymer ligand exchangers

The ATR-FTIR analysis of the chelating ion exchangers TP 220 and M 4195 and their polymeric ligand exchangers e.g. TP 220-Cu and TP 220-CuEDDS as well as M 4195-Cu and M 4195-CuEDDS was performed in order to confirm the presence of functional groups and their successful modification (Fig. 2). The analyses were conducted also after the ClO_4^- sorption. The obtained ATR-FTIR spectra are similar at room temperature due to the presence of the same bis(picolylamine) groups and polystyrene matrix. They show a broad band between 3700 cm^{-1} and 3160 cm^{-1} with the maximum located about 3420 cm^{-1} which is associated with stretching vibrations of the −OH group. The peak 3047 cm^{-1} is assigned to the asymmetric stretching vibrations of −C−H and all the bands 2800-3000 cm^{-1} are characteristic of the polystyrene structure. The peaks at 3014 cm^{-1}, 2911 cm^{-1} are connected with the asymmetric and at 2837 cm^{-1} symmetric stretching vibrations of CH_2 group. The presence of water in the ion exchanger is confirmed by the band at 1618 cm^{-1} which is associated with the vibrations of −OH groups. The bands at 1590 cm^{-1} and 1474 cm^{-1} are associated with the ring stretching vibrations C=C while those at 1433 cm^{-1} and 1362 cm^{-1} with the scissoring vibrations $-CH_2$. The deformation vibrations of 1,4-disubstituted benzene ring were also recorded at 987 cm^{-1} and 833 cm^{-1} (Kołodyńska et al., 2008; Wołowicz and Hubicki, 2012). The band 766 cm^{-1} is assigned to the ring bending vibrations (Kanagathara et al., 2013).

ATR-FTIR spectra of the studied ion exchangers before and after sorption of perchlorate ions change slightly. The most significant change was the appearance of the peak at 1085 cm^{-1} associated with the asymmetric stretching vibrations which show the presence of perchlorate ions (Kanagathara et al., 2013). Also after the sorption, the intensity of some bands changed and the absorbance of peaks was

greater than before the sorption process.

Nitrogen adsorption/desorption measurements of each examined resin before and after the perchlorate ions sorption characterize IV type isotherm according to the IUPAC classification. This type of isotherm indicates the presence of hysteresis loop which points out to the capillary condensation in the mesopores and macropores. The Langmuir type of isotherm (I type) with the same adsorption and desorption curves typical of microporous materials was obtained at low relative pressure while at high relative pressure the hysteresis loop is present and its shape is known to be H1 type. This indicates the presence of cylindrical pores. Fig. 3 shows the examples of the nitrogen adsorption/desorption measurements for TP 220, TP 220-Cu and TP 220-CuEDDS. The pore size distribution of TP 220, TP 220-Cu and TP 220-CuEDDS suggests the superiority of micropores and also indicates occurrence of mesopores and macropores. As for M 4195, M 4195-Cu and M 4195-CuEDDS only mesopores and macropores are present. The obtained results indicate that after sorption of ClO_4^- ions on TP 220, TP 220-Cu and TP 220-CuEDDS the S_{BET} value increased. For example, for TP 220 it was 20.0 m^2/g before sorption and 25.3 m^2/g after sorption.

In order to determine pH dependent the surface charge of TP 220, TP 220-Cu and TP 220-CuEDDS as well as M 4195, M 4195-Cu and M 4195-CuEDDS the potentiometric titration and drift method were applied. According to the potentiometric method, the samples were dispersed in the aqueous media at three ionic strengths and titrated using acid or base solutions whereas in the drift method after the 24-h equilibration, the shift in pH values was measured to calculate the zero point of charge (ZPC). Fig. 4 shows the titration curves for TP 220, TP 220-Cu and TP 220-CuEDDS as well as M 4195, M 4195-Cu and M 4195-CuEDDS which corresponds to the pH_{zpc} values 2.41, 2.50 and 3.80 as well as 3.00, 3,00 and 3.20, respectively regardless of ionic

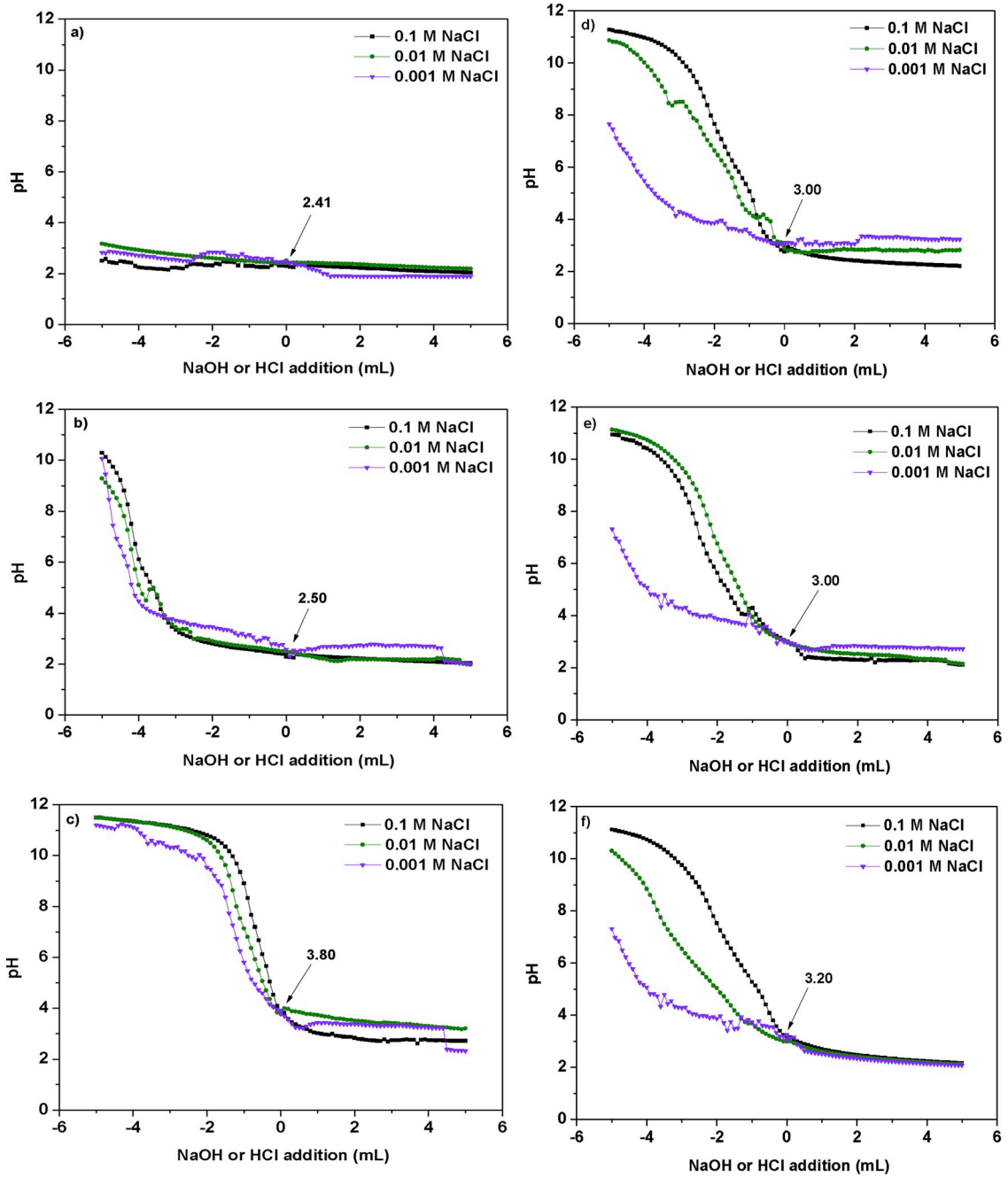

Fig. 4. Surface titration of a) TP 220, b) TP 220-Cu, c) TP 220 Cu-EDDS, d) M 4195 e) M 4195-Cu and f) M4195-CuEDDS at 0.1 M, 0.01 M and 0.001 M NaCl.

strength. In the case of the drift method in 0.01 M NaCl these values were 2.3, 2.4, 3.68 and 2.83, 2.87, 3.03, respectively. The obtained results are almost comparable. When pH was lower than the pH_{zpc} the surface of adsorbents was positively charged, which points out to the anion adsorption by electrostatic attraction. However, when the pH was higher than pH_{zpc}, the surface was negatively charged, so the perchlorate removal was the unfavourable process. The experimental results show that the effective removal of perchlorate is at pH equal to 7 and this can be explained by the fact that the sorption is due to different interactions (inner sphere complex) rather than the electrostatic interactions.

In the next step the TG/DTG analysis of sorbents was made. The heating rate was 10 °C/min up to 1000 °C in the nitrogen atmosphere. The sample weight was between 14.72 and 23.47 mg. On the TG curves the extent of lost or gained weight during heating can be observed. For more accurate interpretation of TG curves, the thermogravimetric (DTG) curves are registered. As a result, the first derivative of the thermogravimetric curve refers to the temperature. The thermogravimetric curves of TP 220, TP 220-Cu and TP 220-CuEDDS as well as M 4195, M 4195-Cu and M 4195-CuEDDS are shown in Fig. 5. The mass

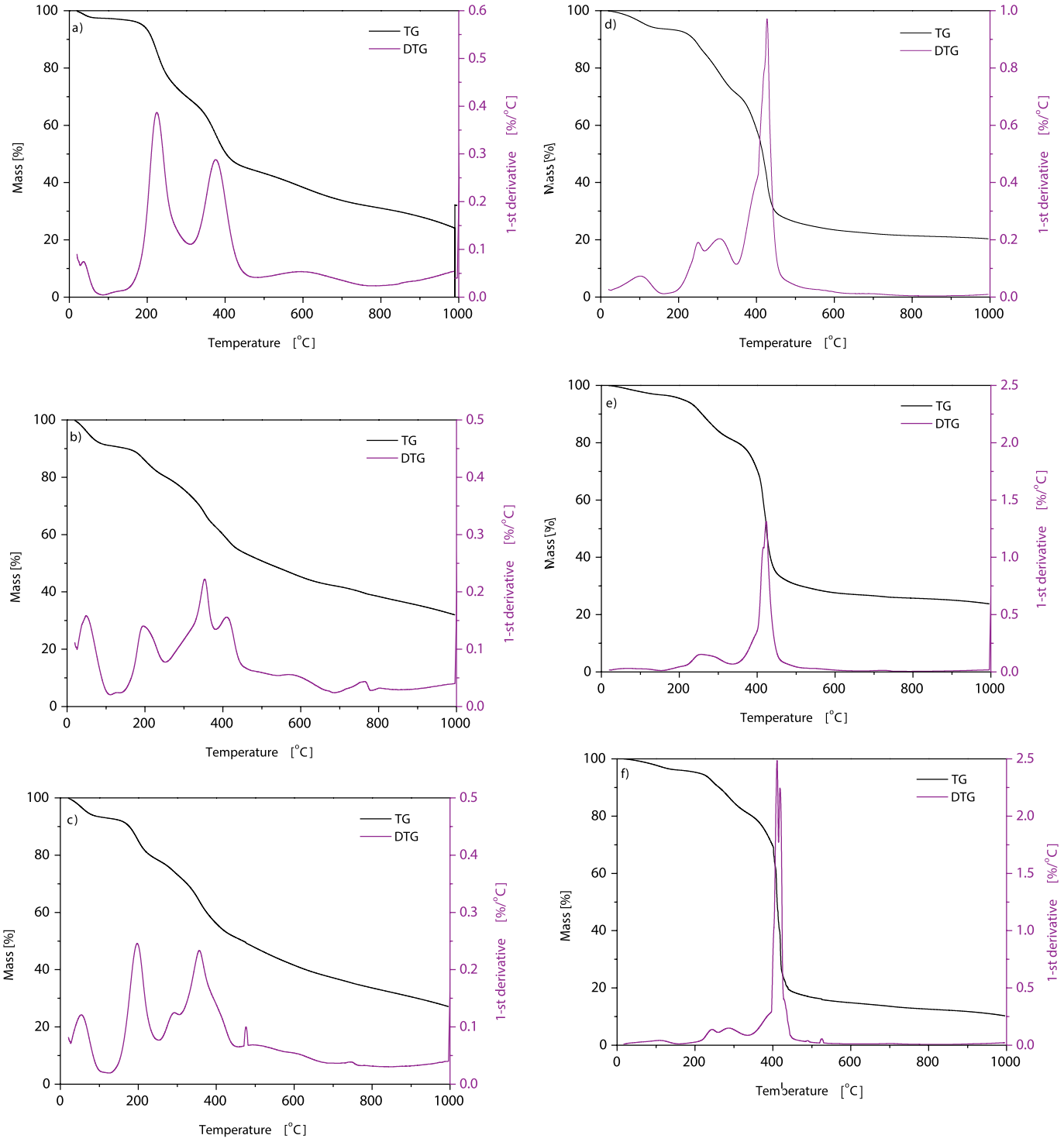

Fig. 5. TG/DTG curves of a) TP 220, b) TP 220-Cu, c) TP 220-CuEDDS, d) M 4195, e) M 4195-Cu and f) M 4195-CuEDDS.

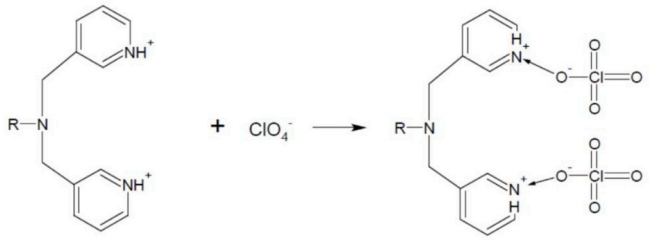

Scheme 1.

losses of the studied resins were as follows: 74%, 66%, 71%, 80%, 75% and 89%, respectively. The shape of the DTG curves indicates that the decomposition reactions of TP 220, TP 220-Cu and TP 220-CuEDDS are complex. However, for M 4195, M 4195-Cu, M 4195-CuEDDS distribution takes place in two main stages. The first one is related to the water loss in the case of each resin. For TP 220, TP 220-Cu and TP 220-CuEDDS it completed at 100 °C, whereas for M 4195, M 4195-Cu and M 4195-CuEDDS at 140 °C. The temperature of maximum decomposition rate for M 4195, M 4195-Cu and M 4195uEDDS was about 420 °C while for TP 220, TP 220-Cu and TP 220-CuEDDS it was observed in two different stages at about 250 and 390 °C. It is known that during the ion exchange resins heating at high temperatures, chemical bonds of polymeric chains break. The first step is related to the presence of polystyrene (29% of the polymer). However, the other one especially in the presence of EDDS complexes is difficult to recognize.

3.2. Sorption mechanism

TP 220 and M 4195 are weak basic chelating ion exchangers with the bis(picolylamine) functional groups and a polystyrene matrix. At the pH value equal to 7 the amine groups of the resin are protonated which indicates enhanced electrostatic interactions (Scheme 1). Xiong et al. pointed out that after Cu(II) loading M 4195 caused an increase in the capacity and separation factors (Scheme 2). This indicates that the addition of positive charges of Cu(II) ions causes an increase in the perchlorate uptake and also the extension of the Lewis acid-base and ion-pairing interactions according to the equations (Xiong et al., 2007):

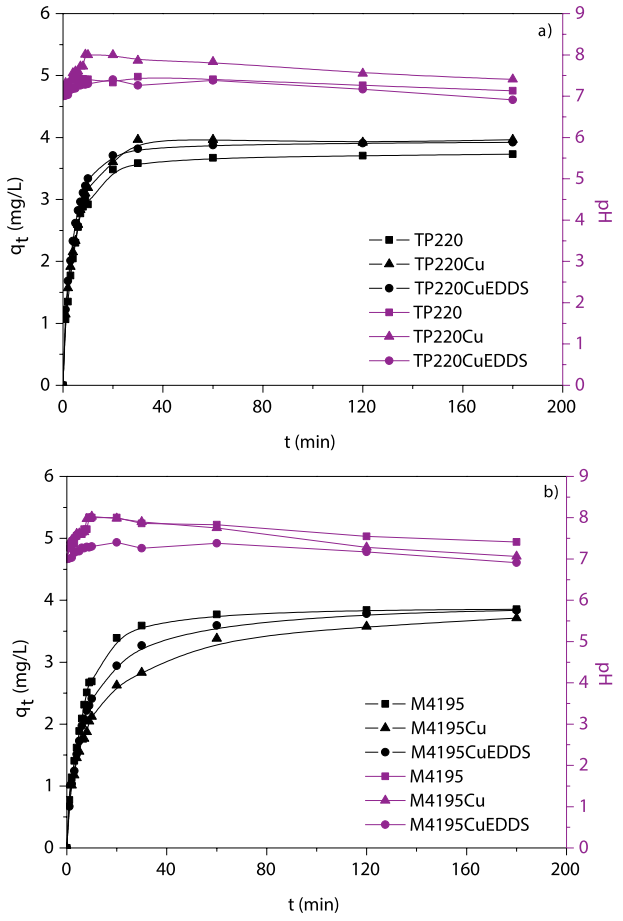

Fig. 6. Effects of the phase contact time on the sorption capacities and pH of perchlorate on a) TP 220, TP 220-Cu and TP 220-CuEDDS, b) M 4195, M 4195-Cu and M 4195-CuEDDS.

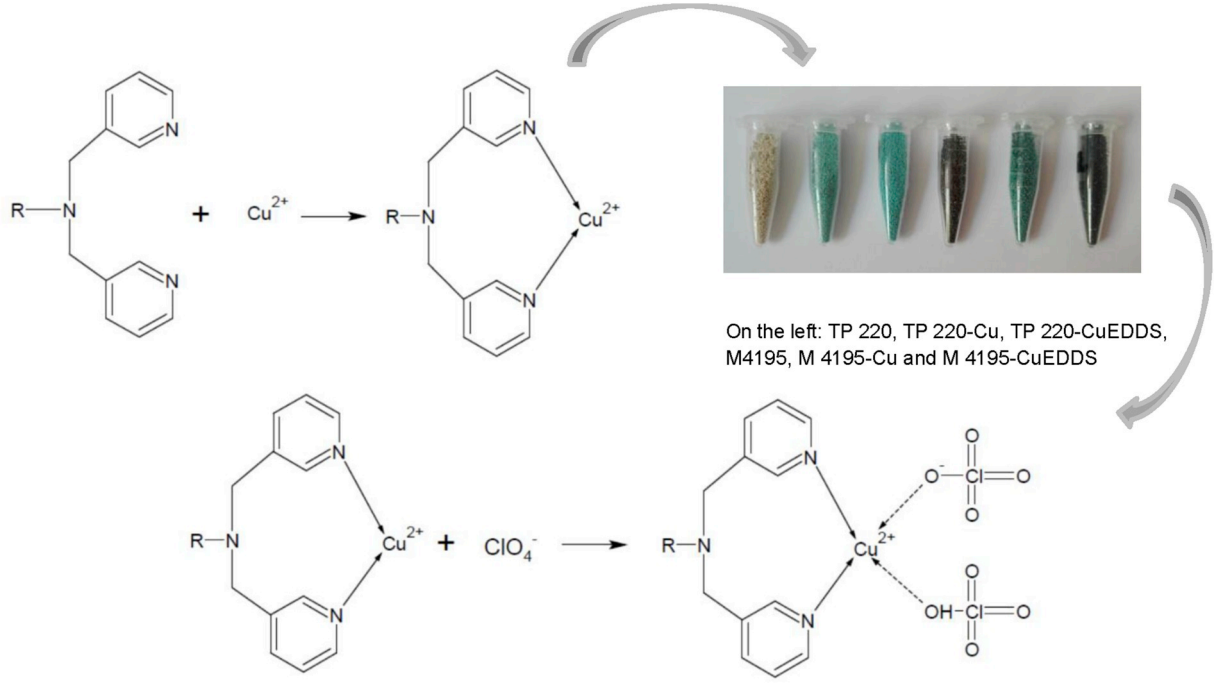

Scheme 2.

Table 2
Kinetic parameters obtained for TP 220, TP 220-Cu and TP 220-CuEDDS.

Model	Parameter	TP 220	TP 220-Cu	TP 220-CuEDDS
PFO	k_1 (1/min)	0.065	0.159	0.071
	q_e (mg/g)	3.73	3.97	3.92
	$q_{e,cal}$ (mg/g)	1.79	3.10	1.71
	R^2	0.888	0.843	0.883
PSO	k_2 (g/mg min)	0.093	0.087	0.110
	q_e (mg/g)	3.73	3.97	3.92
	$q_{e,cal}$ (mg/g)	3.81	4.05	4.00
	R^2	0.999	0.998	0.999
BM	B (1/min)	0.0034	0.0030	0.0039
	D_i (cm^2/min)	2.56×10^{-7}	2.27×10^{-7}	2.96×10^{-7}
	R^2	0.88851	0.8428	0.8836
IPD	k_i (mg/g $min^{1/2}$)	0.788	0.980	1.001
	C (mg/g)	0.651	0.194	0.324
	R^2	0.979	0.993	0.989
FD	K_f (1/min)	4.982	4.483	5.694
	R^2	0.888	0.843	0.883
D-W	K (1/min)	−0.0597	−0.1530	−0.0661
	R^2	0.917	0.837	0.908
Diffusion coefficients	D_p	4.96×10^{-7}	7.03×10^{-9}	9.38×10^{-9}
	D_f	1.24×10^{-6}	1.30×10^{-6}	1.62×10^{-6}

Table 3
Kinetic parameters obtained for M 4195, M 4195-Cu and M 4195Cu-EDDS.

Model	Parameter	M 4195	M 4195-Cu	M 4195-CuEDDS
PFO	k_1 (1/min)	0.063	0.035	0.043
	q_e (mg/g)	3.85	3.71	3.8388
	$q_{e,cal}$ (mg/g)	2.49	2.53	2.55
	R^2	0.948	0.977	0.948
PSO	k_2 (g/mg min)	0.045	0.043	0.041
	q_e (mg/g)	3.85	3.71	3.84
	$q_{e,cal}$ (mg/g)	4.14	3.63	3.94
	R^2	0.998	0.991	0.999
BM	B (1/min)	0.0038	0.0021	0.0028
	D_i (cm^2/min)	2.89×10^{-7}	1.60×10^{-7}	2.11×10^{-7}
	R^2	0.948	0.977	0.948
IPD	k_i (mg/g $min^{1/2}$)	1.064	0.614	0.899
	C (mg/g)	0.510	0.173	0.290
	R^2	0.998	0.956	0.992
FD	K_f (1/min)	5.562	3.310	4.192
	R^2	0.948	0.977	0.948
D-W	K (1/min)	−0.0422	−0.0224	−0.0295
	R^2	0.971	0.994	0.981
Diffusion coefficients	D_p	4.69×10^{-7}	3.52×10^{-7}	4.69×10^{-7}
	D_f	1.00×10^{-6}	6.72×10^{-7}	9.44×10^{-7}

3.3. Kinetic and diffusion models for perchlorate sorption

Fig. 6 presents the effects of contact time on the sorption capacities and pH of perchlorate for all studied adsorbents. The equilibrium time is reached after 30 min. During the contact time the values of pH do not change significantly. Of all studied adsorbents TP 220-Cu proved to be the most effective. Based on those results the kinetic parameters were determined.

Adsorption kinetics depends on the physical and/or chemical characteristics of the adsorbent materials which affect reaction pathways and rates. In order to study adsorption mechanism the PFO, PSO, IPD, BM, D-W models were used and the parameters D_f and D_p were also determined. The obtained kinetic parameters are summarized in Tables 2 and 3.

The PFO model is expressed by Eqs. (3)–(5). Figs. 7a and 8a show the plots of $log(q_e\text{-}q_t)$ vs. t. The obtained results indicate that the pseudo first order constant k_1 increased with the order: TP 220 < TP 220-CuEDDS < TP 220-Cu and M 4195-Cu < M 4195-CuEDDS < M 4195. It can be also concluded that there was a considerable difference between the calculated $q_{e,cal}$ values and the experimental q_e.

The PSO is presented in Eqs. (5)–(7). Figs. 7b and 8b show the plots t/q_t vs. t. The results in Tables 2 and 3 show that the pseudo second constant k_2 increased with the order TP 220-Cu < TP 220 < TP 220-CuEDDS and M 4195-CuEDDS < M 4195-Cu < M 4195. The correlation coefficients (R^2) are much higher than those for the PFO model and the calculated $q_{e,cal}$ values are comparable with the experimental ones for both groups of adsorbents. Xu et al. studied perchlorate removal using the granular activated carbon impregnated by different iron salts. All experimental data were better fitted to the PSO than PFO model (Xu et al., 2016). Also the results presented by Xie et al. confirmed that perchlorate sorption on the cross-linked quaternary chitosan occurs with the PSO model (Xie et al., 2012).

In order to get to know the actual slowest step in the adsorption process, the Boyd plots are presented in Figs. 7c and 8c for perchlorate adsorption onto TP 220, TP 220-Cu, TP 200-CuEDDS and M 4195, M 4195-Cu, M 4195-CuEDDS. According to this model the pore diffusion controls the mass transfer when the plot is linear and passes through the origin. However, when the plot is linear or non-linear and does not pass through the origin, the rate is controlled by the film diffusion or chemical reaction. From the figures it can be concluded that the plots are linear but do not pass through the origin. Therefore the rate is controlled by the film diffusion or the chemical reaction (Arthy and Saravanakumar, 2013; Viegas et al., 2014).

The IPD and FD models were also applied to describe the diffusion mechanism. Figs. 7f and 8f show the plots of q_t vs. $t^{1/2}$, whereas Figs. 7d and 8d present the plot $\ln(1\text{-}q_t/q_e)$ vs. t. For all studied adsorbents straight line plots not passing through the origin were obtained. This deviation from the origin might be influenced by the difference in the rate of mass transfer in the initial and final stages of adsorption process. The parameter obtained from the intraparticle diffusion model showed the increasing adsorption rate (K_i) from 0.788 to 1.001 in the order TP 220 < TP 220-Cu < TP 220-CuEDDS and from 0.614 to 1.064 in the order M 4195 < M 4195-CuEDDS < M 4195-Cu. However, the boundary layer thickness (C) increases from 0.194 to 0.651 in the order TP 220-Cu < TP 220-CuEDDS < TP220 and from 0.173 to 0.510 in the order M 4195-Cu < M 4195-CuEDDS < M 4195. The results obtained by Seliem et al. show that diffusion is not the only rate limiting step in the perchlorate adsorption onto MCM-41, MCM-48 and layered organosilica as well as Cloisite 10A (Seliem et al., 2013).

The above results indicate that these two models are useful to describe the adsorption process. Tables 2 and 3 present the correlation coefficients (R^2) of the IPD model. For TP 220, TP 220-Cu and TP 220-CuEDDS they are equal to 0.979, 0.993 and 0.992 whereas for M 4195, M 4195-Cu and M 4195-CuEDDS they are as follows: 0.998, 0.956 and 0.992, respectively. The R^2 values for the FD model on TP 220, TP 220-Cu and TP 220-CuEDDS are 0.888, 0.843 and 0.883 whereas for M 4195, M 4195-Cu and M 4195-CuEDDS they can be as follows: 0.948, 0.977 and 0.948. The obtained results indicate that the adsorption rate controlling step of perchlorate on the studied adsorbents is primary intraparticle diffusion. However, this is not the only factor, film diffusion and chemical sorption could be affected in the adsorption rate controlling step (Bai et al., 2016). Moreover, the film diffusion rates (K_f) change in the range 4.483–5.694 increasing in the order TP 220-Cu < TP 220 < TP220-CuEDDS. While in the second group of adsorbents they are in the range 3.310–5.562 with the increasing order M 4195-Cu < M 4195-CuEDDS < M 4195.

However, the D-W plots that is $log(1\text{-}F)^2$ vs. t (Figs. 7e and 8e) show almost linear curves. The correlation coefficients for TP 220, TP 220-Cu and TP 220-CuEDDS were 0.917, 0.837 and 0.908, respectively. For M 4195, M 4195-Cu and M 4195-CuEDDS they were 0.971, 0.994 and 0.981, respectively. Also the plot does not pass through the origin

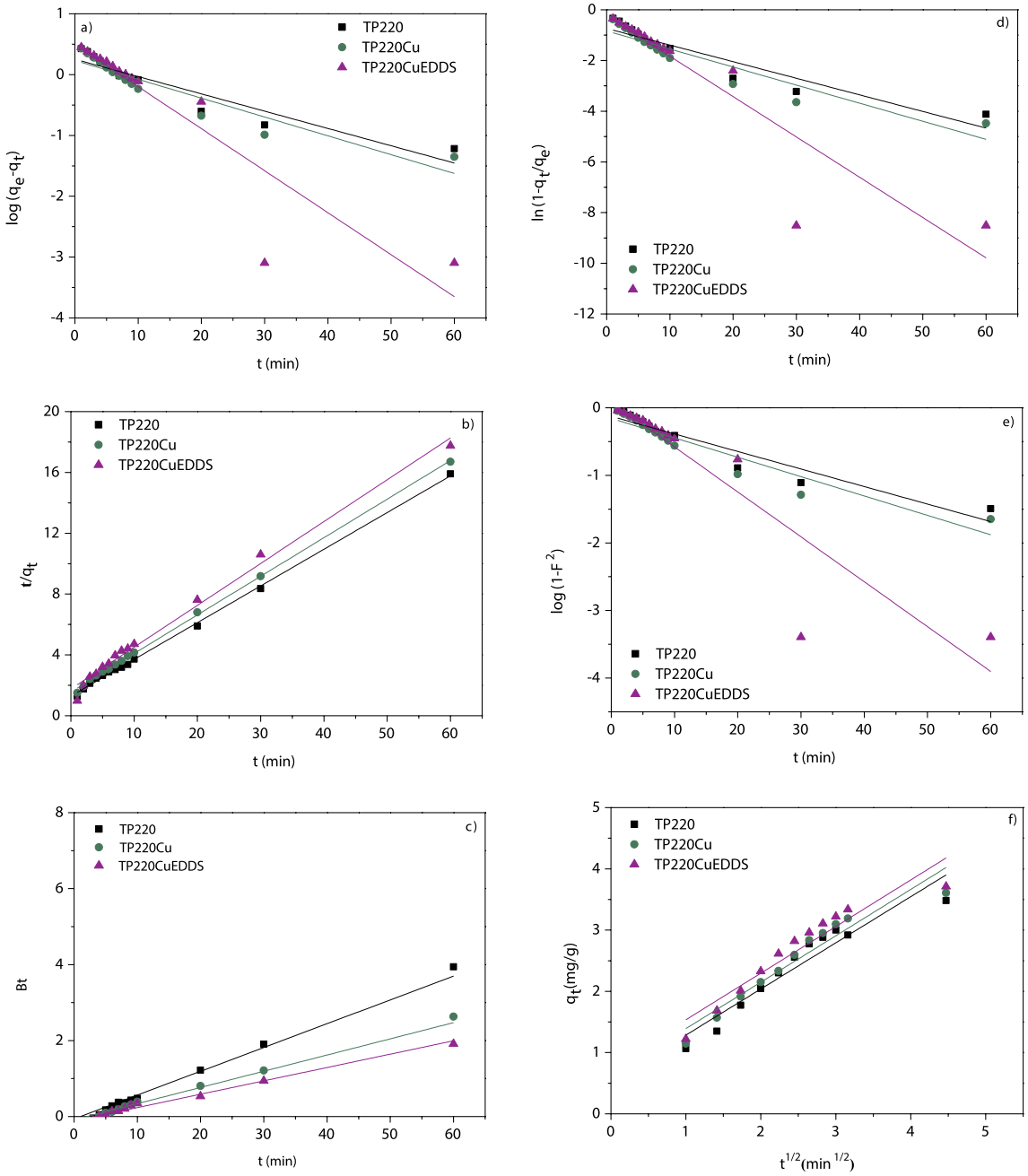

Fig. 7. Kinetic models a) PFO, b) PSO, c) BM, d) FD, e) D-W, f) IPD for TP 220, TP 220-Cu and TP 220-CuEDDS.

which indicates that the diffusion of the adsorbate into pores is not the only rate limiting step. The discussed diffusion models pointed out that the intraparticle model as well as film diffusion and chemical sorption can be the rate controlling step (Hai et al., 2012).

The values of effective diffusion coefficient D_i (cm^2/min) calculated from Eq. (12) are presented in Tables 2 and 3. From the slope of the straight line obtained from the graph *Bt* vs. *t*, the *B* (1/min) values were also calculated.

The pore diffusion coefficient (D_p) and the film diffusion coefficient (D_f) calculated from Eqs. (16) and (17) are presented in Tables 2 and 3. When D_p is in the range 10^{-11} to 10^{-13} cm^2/s, the pore diffusion is the rate controlling step but when D_f is in the range 10^{-6} to 10^{-8} cm^2/s, the film diffusion is the rate controlling step of perchlorate sorption. The values of D_p for all studied adsorbents are not found to be in the order of 10^{-11} to 10^{-13}. However, the parameter D_f for all studied adsorbents in the present study is in the range 10^{-6} to 10^{-8} which indicates that the film diffusion has influence on the rate controlling step (Karthikeyan et al., 2010).

The discussed diffusion models confirmed that the particle diffusion and film diffusion played an important role in controlling the adsorption of perchlorate onto the studied adsorbents. Different results were obtained by Faccini et al. who used the commercially available ion exchange resin CalRes 2109 for perchloarte removal from aqueous solutions. Several kinetic and diffusion models such as the PFO, PSO, Elovich, FD, D-W, W-M and BM were used but only the PSO model was found good enough to fit the experimental results (Faccini et al., 2016b). The comparison of perchlorate sorption on different sorbents is presented in Table 4.

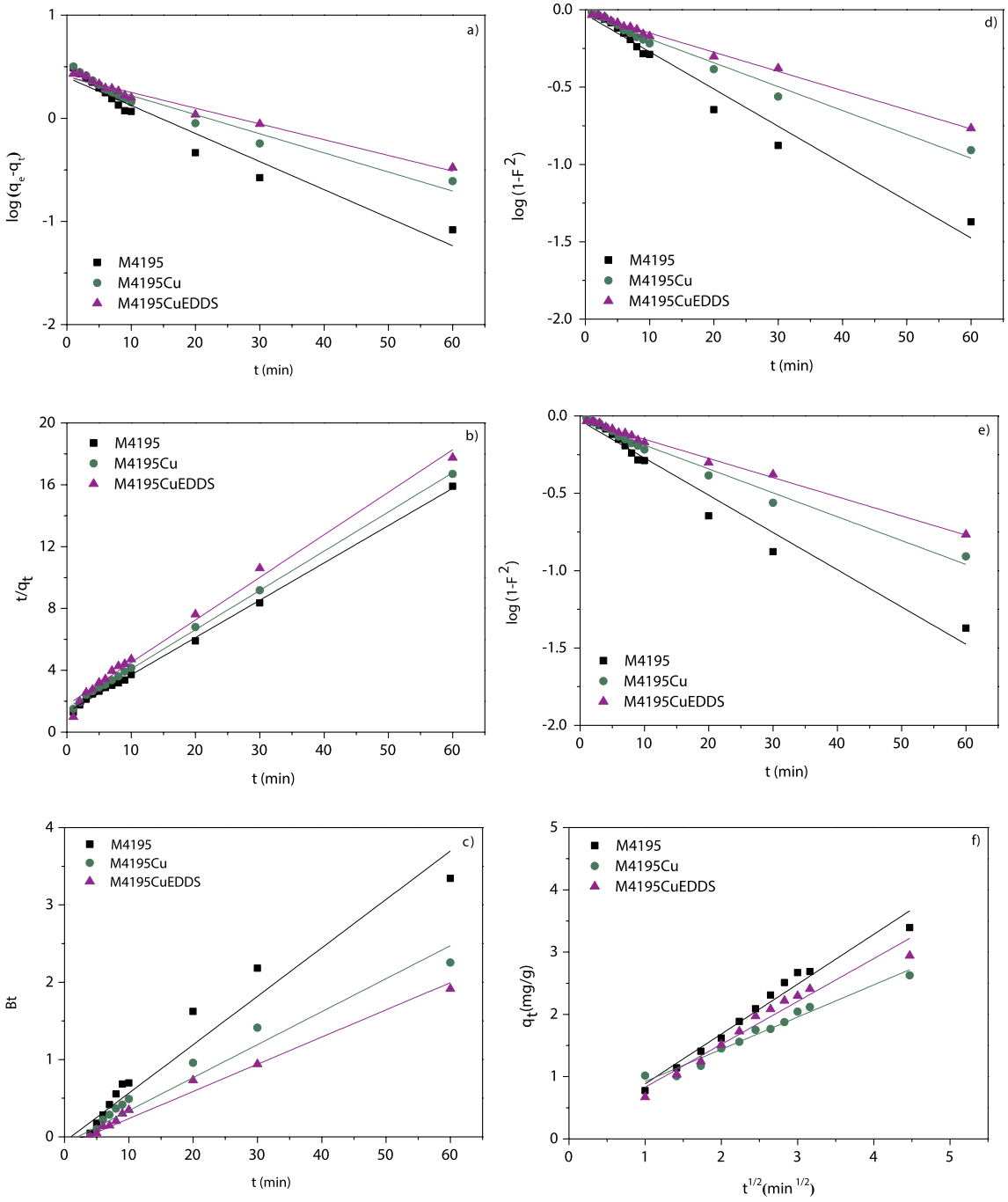

Fig. 8. Kinetic models a) PFO, b) PSO, c) BM, d) FD, e) D-W, f) IPD for M 4195, Dowex M 4195-Cu and M 4195-CuEDDS.

4. Conclusions

In this study PLEs loaded with Cu(II) as well as Cu(II) and EDDS were produced by binding Cu(II) and EDDS onto the commercial ion exchangers TP 220 and M 4195. The paper presents the investigations of perchlorate removal in the presence of Cl^-, Br^-, NO_3^-, PO_4^{3-} and SO_4^{2-} ions from water solution. The obtained results show that the macroporous resins displayed a suitable perchlorate sorption capacity. From the tested adsorbents TP 220-Cu proved to have the greatest perchlorate sorption capacity. The TG/DTG analysis indicates that the decomposition process of ion resins is complex. The hydrophobic nature as well as electrostatic interactions cause that the studied adsorbents are characterized by selectivity for perchlorate removal. The Lewis acid base interactions are very important for those connections between the Cu(II) functional group of PLE and perchlorate. The batch adsorption study illustrates that the pseudo second order model described better the perchlorate adsorption. The experimental results of perchlorate removal indicate that the intraparticle diffusion model and film diffusion were the main adsorption rate controlling factors. As follows from the ATR-FTIR analysis the main adsorption bands also confirmed the presence of perchlorate ions after the sorption process. The nitrogen adsorption desorption analysis pointed out that S_{BET} increased after the perchlorate sorption.

Table 4
Comparison of perchlorate sorption on different sorbents.

Adsorbent	Sorption capacity (mg/g)	pH	References
Commercial sorbents			
SR-7	12.6		Yoon et al. (2009)
IRA900	25	7	(Xiong et al., 2007)
Purolite A530E	90.09	4–10	(Zhu et al., 2015)
Purolite A532E	104.02, 91.00	4–10	(Zhu et al., 2015; Xiong et al., 2007)
MIEX	90.2	4–7	(Zhu et al., 2015)
IRA958	5	7	(Xiong et al., 2007)
DOW-3N	15	7	(Xiong et al., 2007)
DOW-3N—Cu	19	7	(Xiong et al., 2007)
Another sorbents			
ASC	133.5	2–11	(Li et al., 2015)
CM-CS/PVA	8.42	5.9	(Xie et al., 2016b)

Appendix A. Supplementary data

Supplementary data to this article can be found online at https://doi.org/10.1016/j.apgeochem.2018.12.025.

References

Arthy, M., Saravanakumar, M.P., 2013. Isotherm modeling, kinetic study and optimization of batch parameters for effective removal of Acid Blue 45 using tannery waste. J. Mol. Liq. 187, 189–200. https://doi.org/10.1016/j.molliq.2013.06.019.

Asami, M., Yoshida, N., Kosaka, K., Ohno, K., Matsui, Y., 2013. Contribution of tap water to chlorate and perchlorate intake: A market basket study. Sci. Total Environ. 463–464, 199–208. https://doi.org/10.1016/j.scitotenv.2013.05.097.

Bai, H., Zhang, Q., He, T., Zheng, G., Zhang, G., Zheng, L., Ma, S., 2016. Adsorption dynamics, diffusion and isotherm models of poly(NIPAm/LMSH) nanocomposite hydrogels for the removal of anionic dye Amaranth from an aqueous solution. Appl. Clay Sci. 157–166. 124–125. https://doi.org/10.1016/j.clay.2016.02.007.

Diniz, C.V., Ciminelli, V.S.T., Doyle, F.M., 2005. The use of the chelating resin Dowex M-4195 in the adsorption of selected heavy metal ions from manganese solutions. Hydrometallurgy 78, 147–155. https://doi.org/10.1016/j.hydromet.2004.12.007.

El-Khaiary, M.I., Malash, G.F., Ho, Y.S., 2010. On the use of linearized pseudo-second-order kinetic equations for modeling adsorption systems. Desalination 257, 93–101. https://doi.org/10.1016/j.desal.2010.02.041.

Faccini, J., Ebrahimi, S., Roberts, D.J., 2016a. Regeneration of a perchlorate-exhausted highly selective ion exchange resin: Kinetics study of adsorption and desorption processes. Separ. Purif. Technol. 158, 266–274. https://doi.org/10.1016/j.seppur.2015.12.019.

Faccini, J., Ebrahimi, S., Roberts, D.J., 2016b. Regeneration of a perchlorate-exhausted highly selective ion exchange resin: Kinetics study of adsorption and desorption processes. Separ. Purif. Technol. 158, 266–274. https://doi.org/10.1016/j.seppur.2015.12.019.

Flor, G., Vincenzo, M., Riccardi, R., 1974. Kinetics of formation of $SrWO_4$ in the solid state reaction between WO_3 and $SrCO_3$. Z. Naturforsch. 29, 502–506.

Hai, T., Gui-Zhong, L.I.U., You-bin, Y.A.N., Jian-long, G., 2012. Enhancement of removal of organic pollutants from coking wastewater through adsorption by modified coal fly ash. Environ. Protect. Eng. 38, 79–95. https://doi.org/10.5277/EPE120308.

Hendrick, E., Behymer, T.D., Slingsby, R., Munch, D.J., 2005. Method 332.0: Determination of perchlorate in drinking water by ion chromatography with suppressed conductivity and elcectrospray ionization mass spectrometry. EPA Rep 1–48.

Henry, W.D., Zhao, D., SenGupta, A.K., Lange, C., 2004. Preparation and characterization of a new class of polymeric ligand exchangers for selective removal of trace contaminants from water. React. Funct. Polym. 60, 109–120. https://doi.org/10.1016/j.reactfunctpolym.2004.02.016.

Ho, Y.S., Mckay, G., 1998. Kinetic mModels for the sorption of dye from aqueous solution by wood. Process Saf. Environ. Protect. 76, 183–191. https://doi.org/10.1205/095758298529326.

Janin, A., Blais, J.F., Mercier, G., Drogui, P., 2009. Selective recovery of Cr and Cu in leachate from chromated copper arsenate treated wood using chelating and acidic ion exchange resins. J. Hazard Mater. 169, 1099–1105. https://doi.org/10.1016/j.jhazmat.2009.04.066.

Jiang, C., Yang, Q., Wang, D., Zhong, Y., Chen, F., Li, X., Zeng, G., Li, X., Shang, M., 2017. Simultaneous perchlorate and nitrate removal coupled with electricity generation in autotrophic denitrifying biocathode microbial fuel cell. Chem. Eng. J. 308, 783–790. https://doi.org/10.1016/j.cej.2016.09.121.

Kanagathara, N., Marchewka, M.K., Drozd, M., Renganathan, N.G., Gunasekaran, S., Anbalagan, G., 2013. FT-IR, FT-Raman spectra and DFT calculations of melaminium perchlorate monohydrate. Spectrochim. Acta Part A Mol. Biomol. Spectrosc. 112, 343–350. https://doi.org/10.1016/j.saa.2013.04.001.

Karthikeyan, S., Sivakumar, B., Sivakumar, N., 2010. Film and pore diffusion modeling for adsorption of Reactive Red 2 from aqueous solution on to activated carbon Bio-Diesel Industrial Waste. E-Journal Chem. 7, S175–S184. https://doi.org/10.1155/2010/138684.

Khalil, T.E., El-Dissouky, A., Rizk, S., 2016. Equilibrium and Kinetic studies on Pb^{2+}, Cd^{2+}, Cu^{2+} and Ni^{2+} adsorption from aqueous solution by resin 2,2'- (ethylenedithio)diethanol immobilized Amberlite XAD-16 (EDTDE-AXAD-16) with chlorosulphonic acid. J. Mol. Liq. 219, 533–546. https://doi.org/10.1016/j.molliq.2016.03.063.

Kiruba, U.P., Kumar, P.S., Prabhakaran, C., Aditya, V., 2014. Characteristics of thermodynamic, isotherm, kinetic, mechanism and design equations for the analysis of adsorption in Cd(II) ions-surface modified Eucalyptus seeds system. J. Taiwan Inst. Chem. Eng. 45, 2957–2968. https://doi.org/10.1016/j.jtice.2014.08.016.

Kołodyńska, D., 2010. The effects of the treatment conditions on metal ions removal in the presence of complexing agents of a new generation. Desalination 263, 159–169. https://doi.org/10.1016/j.desal.2010.06.053.

Kołodyńska, D., Sofińska-Chmiel, W., Mendyk, E., Hubicki, Z., 2014. Dowex M 4195 and Lewatit® MonoPlus TP 220 in heavy metal ions removal from acidic streams. Separ. Sci. Technol. 49. https://doi.org/10.1080/01496395.2014.908920 2003–2015.

Kołodyńska, D., Ryczkowski, J., Hubicki, Z., 2008. FT-IR/PAS studies of chelates adsorption on anion exchangers. Eur. Phys. J. Spec. Top. 154, 339–343. https://doi.org/10.1140/epjst/e2008-00572-7.

Li, T., Yang, Z., Zhang, X., Zhu, N., Niu, X., 2015. Perchlorate removal from aqueous solution with a novel cationic metal-organic frameworks based on amino sulfonic acid ligand linking with Cu-4,4'-bipyridyl chains. Chem. Eng. J. 281, 1008–1016. https://doi.org/10.1016/j.cej.2015.07.010.

Mendes, F.D., Martins, A.H., 2004. Selective sorption of nickel and cobalt from sulphate solutions using chelating resins. Int. J. Miner. Process. 74, 359–371. https://doi.org/10.1016/j.minpro.2004.04.003.

Nagib, S., Inoue, K., Yamaguchi, T., Tamaru, T., 1999. Recovery of Ni from a large excess of Al generated from spent hydrodesulfurization catalyst using picolylamine type chelating resin and complexane types of chemically modified chitosan. Hydrometallurgy 51, 73–85. https://doi.org/10.1016/S0304-386X(98)00073-5.

Nethaji, S., Sivasamy, A., Mandal, A.B., 2013. Adsorption isotherms, kinetics and mechanism for the adsorption of cationic and anionic dyes onto carbonaceous particles prepared from Juglans regia shell biomass. Int. J. Environ. Sci. Technol. 10, 231–242. https://doi.org/10.1007/s13762-012-0112-0.

Office, E.P.A, 1999. Determination of Perchlorate in Drinking Water Using Ion. Zitat siehe Urbansky 27, 1–49 2002.

Pohl, C., Later, D., Joyce, R., Srinivasan, K., Deborba, B., Thomas, D., 2005. Determination of Perchlorate in Drinking Water Using. pp. 1–38.

Saygi, K.O., Tuzen, M., Soylak, M., Elci, L., 2008. Chromium speciation by solid phase extraction on Dowex M 4195 chelating resin and determination by atomic absorption spectrometry. J. Hazard Mater. 153, 1009–1014. https://doi.org/10.1016/j.jhazmat.2007.09.051.

Seliem, M.K., Komarneni, S., Byrne, T., Cannon, F.S., Shahien, M.G., Khalil, A.A., Abd El-Gaid, I.M., 2013. Removal of perchlorate by synthetic organosilicas and organoclay: Kinetics and isotherm studies. Appl. Clay Sci. 71, 21–26. https://doi.org/10.1016/j.clay.2012.10.008.

Tang, Y., Liang, S., Guo, H., You, H., Gao, N., Yu, S., 2013. Adsorptive characteristics of perchlorate from aqueous solutions by MIEX resin. Colloids Surfaces A Physicochem. Eng. Asp. 417, 26–31. https://doi.org/10.1016/j.colsurfa.2012.10.040.

Tao, W., Li, A., Long, C., Fan, Z., Wang, W., 2011. Preparation, characterization and application of a copper (II)-bound polymeric ligand exchanger for selective removal of arsenate from water. J. Hazard Mater. 193, 149–155. https://doi.org/10.1016/j.jhazmat.2011.07.041.

Urbansky, E.T., 1998. Perchlorate Chemistry: Implications for Analysis and Remediation. Bioremediat. J. 2, 81–95. https://doi.org/10.1080/10889869891214231.

Viegas, R.M.C., Campinas, M., Costa, H., Rosa, M.J., 2014. How do the HSDM and Boyd's model compare for estimating intraparticle diffusion coefficients in adsorption processes. Adsorption 20, 737–746. https://doi.org/10.1007/s10450-014-9617-9.

Wendelken, S.C., Munch, D.J., Pepich, B.V., Later, D.W., Pohl, C.A., 2005. Method 331.0 Determination of perchlorate in drinking water by liquid chromatography electrospray ionization mass spectrometry. EPA Rep 1–34.

Wołowicz, A., Hubicki, Z., 2012. The use of the chelating resin of a new generation Lewatit MonoPlus TP-220 with the bis-picolylamine functional groups in the removal of selected metal ions from acidic solutions. Chem. Eng. J. 197, 493–508. https://doi.org/10.1016/j.cej.2012.05.047.

Xie, Y., Li, S., Liu, G., Wang, J., Wu, K., 2012. Equilibrium, kinetic and thermodynamic studies on perchlorate adsorption by cross-linked quaternary chitosan. Chem. Eng. J. 192, 269–275. https://doi.org/10.1016/j.cej.2012.04.014.

Xie, Y., Wu, Y., Qin, Y., Yi, Y., Diao, Z., Liu, G., Zhou, T., Xu, M., 2016a. Perchlorate degradation in aqueous solution using chitosan-stabilized zero-valent iron nanoparticles. Separ. Purif. Technol. 171, 164–173. https://doi.org/10.1016/j.seppur.2016.07.023.

Xie, Y.H., Wu, Y.L., Qin, Y.H., Yi, Y., Liu, Z., Lv, L., Xu, M., 2016b. Evaluation of perchlorate removal from aqueous solution by cross-linked magnetic chitosan/poly (vinyl alcohol) particles. J. Taiwan Inst. Chem. Eng. 65, 295–303. https://doi.org/10.1016/j.jtice.2016.05.022.

Xiong, Z., Zhao, D., Harper, W.F., 2007. Sorption and desorption of perchlorate with various classes of ion exchangers: A comparative study. Ind. Eng. Chem. Res. 46, 9213–9222. https://doi.org/10.1021/ie0702025.

Xu, J., Gao, N., Zhao, D., Liu, Z., Tang, M., Chen, Y., Zhu, Y., 2016. Different iron salt impregnated granular activated carbon (Fe-GAC) for perchlorate removal: Characterization, performance and mechanism. Colloids Surfaces A Physicochem. Eng. Asp. 509, 99–108. https://doi.org/10.1016/j.colsurfa.2016.08.039.

Yao, F., Zhong, Y., Yang, Q., Wang, D., Chen, F., Zhao, J., Xie, T., Jiang, C., An, H., Zeng, G., Li, X., 2017. Effective adsorption/electrocatalytic degradation of perchlorate using Pd/Pt supported on N-doped activated carbon fiber cathode. J. Hazard Mater.

323, 602–610. https://doi.org/10.1016/j.jhazmat.2016.08.052.
Ye, L., You, H., Yao, J., Su, H., 2012. Water treatment technologies for perchlorate: A review. Desalination 298, 1–12. https://doi.org/10.1016/j.desal.2012.05.006.
Yoon, I.H., Meng, X., Wang, C., Kim, K.-W., Bang, S., Choe, E., Lippincott, L., 2009. Perchlorate adsorption and desorption on activated carbon and anion exchange resin. J. Hazard Mater. 164, 87–94. https://doi.org/10.1016/j.jhazmat.2008.07.123.
Zhang, W., Cheng, C.Y., 2007. Manganese metallurgy review. Part II: Manganese separation and recovery from solution. Hydrometallurgy 89, 160–177. https://doi.org/10.1016/j.hydromet.2007.08.009.
Zhao, D., Sengupta, A.K., 1998. Ultimate removal of phosphate from wastewater using a new class of polymeric ion exchangers. Water Res. 32, 1613–1625. https://doi.org/10.1016/S0043-1354(97)00371-0.
Zhu, H.X., Cao, X.J., He, Y.C., Kong, Q.P., He, H., Wang, J., 2015. Removal of Cu^{2+} from aqueous solutions by the novel modified bagasse pulp cellulose: Kinetics, isotherm and mechanism. Carbohydr. Polym. 129, 115–126. https://doi.org/10.1016/j.carbpol.2015.04.049.
Zhu, Y., Gao, N., Wang, Q., Wei, X., 2015. Adsorption of perchlorate from aqueous solutions by anion exchange resins: Effects of resin properties and solution chemistry. Colloids Surfaces A Physicochem. Eng. Asp. 468, 114–121. https://doi.org/10.1016/j.colsurfa.2014.11.062.